Journal of
Materials Chemistry C

Accepted Manuscript

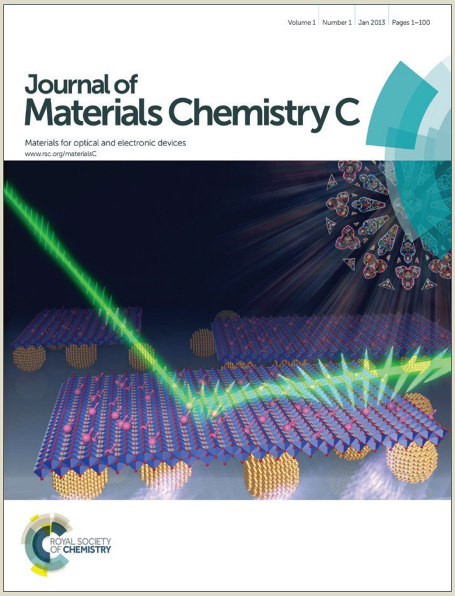

ROYAL SOCIETY
OF **CHEMISTRY**

www.rsc.org/materialsC

Journal of Materials Chemistry C RSCPublishing

ARTICLE

Synthesis, characterization and electrical properties of silicon-doped graphene films

Cite this: DOI: 10.1039/x0xx00000x

Zegao Wang,[abc] Pingjian Li,*[a] Yuanfu Chen,*[a] Jingbo Liu,[a] Wanli Zhang,[a] Zheng Guo,[c] Mingdong Dong,[b] and Yanrong Li[a]

Received 00th January 2012,
Accepted 00th January 2012

DOI: 10.1039/x0xx00000x

www.rsc.org/

Theoretical calculations have predicted that silicon doping can modifies the electronic structure of graphene; however, it is difficult to synthesize high-quality silicon doped graphene (SiG), thus the electrical properties of SiG have still remained unexplored. In this study, monolayer SiG film was synthesized by chemical vapour deposition using triphenylsilane ($C_{18}H_{15}Si$) as the sole solid source, which provides both carbon and silicon atoms. The silicon doping content is ~ 2.63 at%, and silicon atoms are incorporated into graphene lattice with pure Si-C bonds. Furthermore, electrical studies reveal that the as-synthesized SiG film shows a typical p-type doping behaviour with a considerably high carrier mobility of about 660 cm^2/Vs at room temperature. In addition, due to the single doping structure of Si–C bonds, the SiG film can be expected to be used as an excellent platform for studying silicon doping effects on the physical and chemical properties of graphene.

Introduction

Graphene has attracted a great deal of attention due to its extraordinary electronic properties, such as high mobility, room-temperature quantum Hall effect and the modulated bipolar field effect characteristics.[1-4] For pristine graphene (PG), the valence and conduction band of graphene intersects at K point, which reveals that graphene is a zero-gap semiconductor.[5,6] Recently, it has been demonstrated that electronic band structure of graphene can be stably modulated by heteroatom doping, which will tailor its electrical and chemical properties.[7-9]

Until now, it has been reported that nitrogen, boron and sulfur atoms can be successfully doped into graphene and modulate its electrical and chemical properties.[10-15] Besides above heteroatom doping, theoretic research shows that the silicon (Si) doping can also remarkably modulated the electronic structure of graphene, which may open a band gap or enhance the catalytic performance of graphene.[16-21] However, it is difficult to dope silicon atoms into graphene lattice with stable Si-C bonds, because the atomic radius of silicon atom (117 pm) is much larger than that of carbon atom (77 pm).

Recently, some groups directly experimentally monitored silicon atom in unintentional doped graphene,[22-24] which revealed that silicon atoms can stably incorporated into graphene lattice. Most recently, Lv et al. reported the chemical vapour deposition (CVD) synthesis of Si-doped graphene (SiG).[25] However, the electrical properties of SiG have still remained unexplored. In addition, it is noted that, for the work reported in Ref. 25, the SiG film has two types of Si-bonding configurations (Si-C and Si-O). It hinders a conclusive study of Si doping effect on the physical and chemical properties of graphene, because the different types of Si-bonding configurations may correspond to different properties. Thus, it is still a challenge to synthesize SiG film with pure Si-bonding configurations.

In this study, monolayer SiG film has been synthesized by using triphenylsilane ($C_{18}H_{15}Si$) as the sole solid source, which can provide not only the carbon atoms, but also silicon atoms. Silicon atoms are successfully doped into graphene lattice with pure Si-C bonds, and the silicon content is ~ 2.63 at%. Furthermore, electrical studies reveal that as-synthesized SiG film shows a p-type doping behaviour, and its mobility is ~ 660 cm^2/Vs, which can be comparable to that of boron-doped graphene.[13] According to our knowledge, it is the first time to use the sole source of both carbon and silicon for growing SiG film with pure Si-C bonds, and investigate its electrical properties.

Experimental

Synthesis of SiG film. The SiG film was synthesized by using the CVD method as follows. Firstly, 25-μm-thick Cu foil (Alfa Aesar, item no. 13382) used as growth substrate was loaded into the hot center inside the tube furnace, and a ceramics container with ~ 100 mg triphenylsilane used as the sole source was placed outside the hot zone, as shown in Figure 1. Secondly, the system was evacuated with a vacuum background of lower than 1×10^{-3} Pa, and then the Cu foil was annealed at 1050 ^oC in a 30 sccm H_2 and 50 sccm Ar for 20 min for removing its surface oxide layer. Thirdly, the temperature of Cu foil was decreased to the growth temperature (800 ^oC), and then the triphenylsilane was mildly sublimated with the heating belt at 100 ^oC by using the heating belt; the growth time was ~30 min, and the flux of H_2 and Ar remained unchanged. Finally, the system was cooled to room temperature with a cooling rate of 50 ℃ /min in H_2/Ar ambience.

Synthesis of PG film. The PG film was synthesized on the Cu foil by using the common CVD method, where CH_4 was used as carbon source. The detailed process can be seen in our previous work.[4]

Transfer process of SiG and PG films. For characterizations and measurements, SiG and PG films were transferred onto the target substrates by using PMMA as the supporting layer. The detailed process can be seen in our previous work.[4]

Characterizations. X-ray photoelectron spectroscopy was performed on a Kratos XSAM800 using Al Ka radiation (144 W, 12 mA, 12 kV). The silicon doping content is calculated by $Si/C=(A_{Si}/S_{Si2p})/(A_C/S_{C1s})$, where A_{Si} and A_C are the area of Si2p and C1s peaks, S_{Si2p} and S_{C1s} are the corresponding sensitive factors. The high-resolution transmission electron microscope image was taken with an FEI Tecnai G2 microscope. Raman spectroscopy was performed on a Renishaw Spectrometer (514 nm). The Kelvin probe force microscope (KPFM) was measured using Bruker Dimension Icon, and the Co/Cr tip was employed to test the contact potential difference between tip and film; the lift-height of tip was 5 nm.

Device fabrication and electrical measurements. For electrical measurements, the field-effect transistors were fabricated by using standard photolithography after transferring the SiG or PG film onto the 300 nm SiO_2/Si substrate. The Ti/Au (30/50 nm) film was deposited as source and drain electrodes; the 300 nm SiO_2 and n++ silicon layers acted as the gate dielectric and back-gate electrode, respectively. The electrical measurements were carried out with an Agilent 4155B semiconductor parameter analyzer in air at room temperature.

Results and discussion

Figure 1 shows the schematic illustration for the synthesis of SiG film on Cu foil by CVD method, where triphenylsilane was used as the sole solid source, which provide both carbon and silicon atoms. For comparison, the PG film was also synthesized by the common CVD method, which was reported in our previous work.[4]

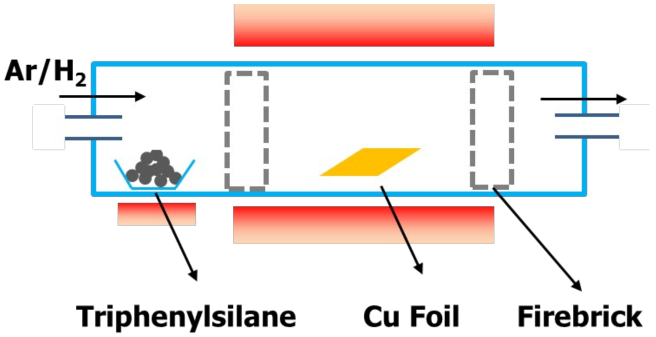

Fig. 1 Schematic illustration for the CVD synthesis of SG film by using triphenylsilane as the sole carbon and silicon source.

In order to study the silicon doping content and configuration, the X-ray photoelectron spectroscopy (XPS) measurements were performed after transferring the SiG films onto the sapphire substrate. As shown in Figure 2a, compared with sapphire substrate, C1s peaks appear in the XPS spectra of SiG and PG films, which correspond to the carbon atoms of graphene. Figure 2b shows the high-resolution Si2p XPS spectra of SiG and PG films. One can observer that the Si2p peak appears in the XPS spectrum of SiG film, which indicates that silicon atoms are incorporated into graphene. Furthermore, the Si2p peak can be deconvoluted into two peaks at binding energies of ~ 101.1 eV and ~ 102.0 eV, which correspond to the $Si2p_{3/2}$ and $Si2p_{1/2}$ energy positions of Si-C, respectively.[26-28] More significantly, other Si components cannot be detected, such as Si-O at around 103~105 eV reported in Ref. 25. The SiG film with pure Si-bonding configurations can serve as an excellent platform to study doping effects of the physical and chemical properties of graphene.

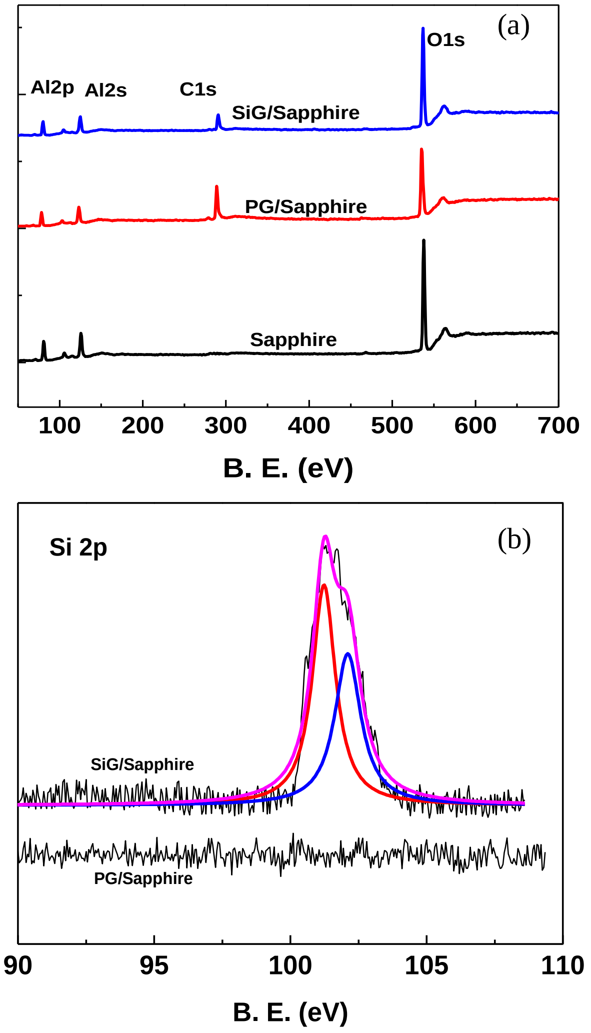

Fig. 2 (a) XPS spectra of sapphire, PG/sapphire and SiG/sapphire. (b) High resolution Si 2p XPS spectra of SiG and PG films transferred onto sapphire substrates.

Furthermore, from XPS spectra shown in Figure 2a, one can observe that the C/O atom ratio of SiG film is higher than that of PG. It is noted that O peaks for SiG and PG film are mainly originated from the sapphire substrates. However, considering the same substrate effect for both SiG and PG film, the higher C/O atom ratio of SiG film corresponds to the higher O content of SiG film than that of PG film. On the other hand, the possibility of Si-O formation can be excluded from the XPS studies shown in Figure 2b. Therefore, we can conclude that silicon doing causes the more absorption of O_2 molecules on graphene film. It implies that doped Si-C structures in graphene have low absorption energy for gas molecules, and SiG film can be used as an excellent candidate for gas detection.[29,30] In addition, the Si content (Si/C) of as-synthesized SiG film is ~

2.63 at%, which is comparable to that of SiG reported in Ref 25 (~ 1.75 at%) and silicon doped reduced graphene oxide reported in Ref. 31.

In order to investigate the microstructure of SiG film, transmission electron microscope (TEM) was used. Figure 3a shows the high-resolution TEM image of random edge of SiG film, indicating monolayer structure. Furthermore, the uniformity of monolayer SiG film was investigated by measuring the optical transmittances. As shown in Figure 3b, at 550 nm, the SiG film has an optical transmittance of ~ 96.7%, which is very close to that of PG film (97.0%). It implies that the as-synthesized monolayer SiG film has high uniformity.

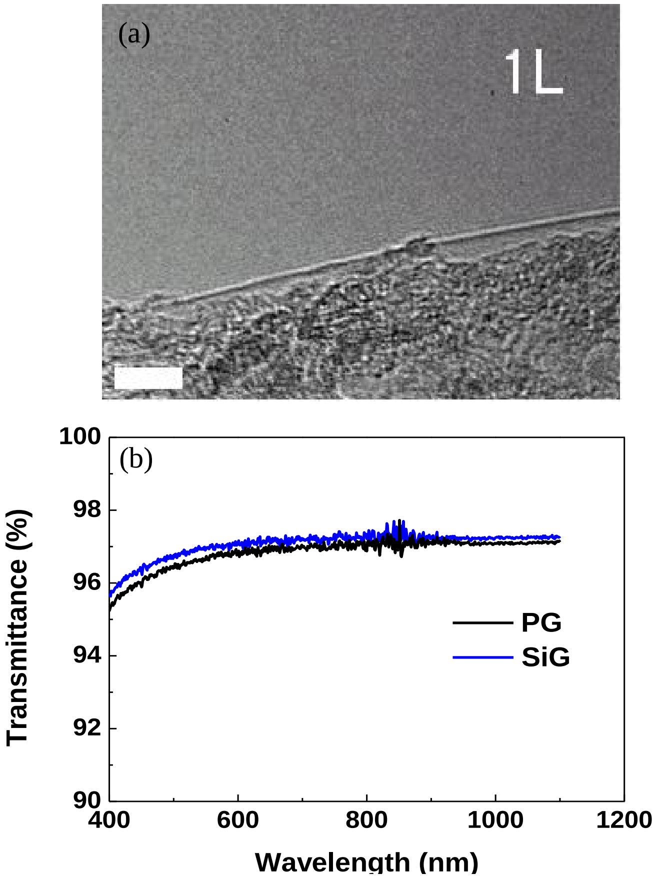

Fig. 3 (a) HRTEM image of SiG film. The bar is 5 nm. (b) UV-vis transmittance spectra of SiG and PG films transferred onto PET substrates.

Raman spectroscopy was used for further studying the structure properties of SiG films. Figure 4a shows the typical Raman spectra of SiG and PG films transferred onto SiO_2/Si substrates. Compared with PG film, a new band (G', ~ 1623 cm^{-1}) near the G band appears and the intensity of 2D band decreases with respect to that of G band for SiG film, which were also observed in reported heteroatom doped graphene films.[10-14] More significantly, our Raman studies reveal that silicon doping causes the increase of 2D band position from 2687.5 cm^{-1} to 2691.3 cm^{-1}, and the increase of the G band position from 1585.0 cm^{-1} to 1593.9 cm^{-1}. Previous reports demonstrated that p-type doping caused the upshifts of both 2D and G band positions; in contrast, n-type doping caused the downshift of 2D band position and upshift of G band position.[13,32] So we can conclude that silicon doping is p-type doping. Further, the doping hole concentration can be estimated from the Raman shift of G band position (~8.9 cm^{-1}), and the corresponding value is ~ 1.2×10^{13} cm^{-2}.[33]

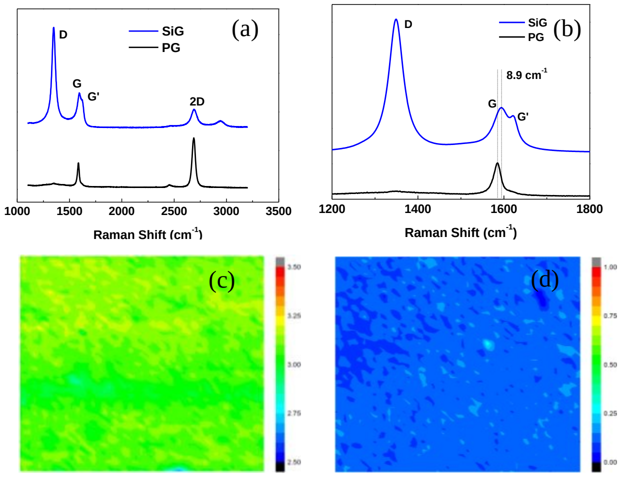

Fig. 4 (a) Typical Raman spectra of SiG and PG films transferred onto SiO_2/Si substrates. (b) Enlarged D and G bands of SiG and PG films. Raman mapping of I_D/I_G of (c) SiG and (d) PG at the 50×50 μm^2 scale, respectively.

In addition, from Raman spectra shown in Figure 4b, we also noticed that after silicon atoms are doped into the graphene, the D band intensity of SiG film rises rapidly. This is due to the structural defects induced by silicon doping, including doped silicon atoms, bonding disorders and vacancies in the graphene lattice.[10-14] Furthermore, previous report demonstrated that the crystallite size (L_a) of graphene can be estimated from $L_a = (2.14\times10^{-10})\lambda^4(I_D/I_G)^{-1}$,[34] where λ is the wavelength (514 nm), and I_D/I_G is the ratio of D to G bands intensities). From the Raman mapping of I_D/I_G of SiG and PG film shown in Figure 4c and 4d (50×50 μm^2), the average values of ID/IG for SiG and PG are ~ 3.19 and ~ 0.13, which correspond to crystallite size of ~ 5 nm and ~ 129 nm, respectively. It indicates that the silicon doping causes the decrease of the crystallite size of graphene. The similar phenomena have also observed in other heteroatom doped graphene films reported previously.[32,35]

For further studying the electronic structure of SiG films, Kelvin probe force microscopy (KPFM) was used to study the work function by measuring the contact potential difference between the tip and films, as shown in Figure 5. During the KPFM scanning, the topography of film will be recorded in the first pass, and then the voltage difference between tip and film will be recorded in the second pass. Actually, the recorded voltage difference is the contact potential difference (V_{cpd}), which is given by $V_{cpd} = (\varphi_{tip} - \varphi_{film})/e$, where φ_{tip} and φ_{film} are the work function of tip and film, respectively.[36] Thus, the work function of film could be given by $\varphi_{film} = \varphi_{tip} - eV_{cpd}$, and the variation of work function can be expressed by $\Delta\varphi_{film} = -e\Delta V_{cpd}$, which is independent of the tip. Figure 5a shows the topography of SiG film. Figure 5b and 5c show the surface potential maps of SiG and PG films, respectively. Figure 5d shows the histogram of surface potential. One can see that the contact potential difference decreases by ~ 232 mV, which shows the work function increases and the Fermi energy downshifts by 232 meV after doping silicon. Therefore, one can conclude that silicon doping shows p-type doping characteristics, corresponding to the downshift of Fermi energy.[37]

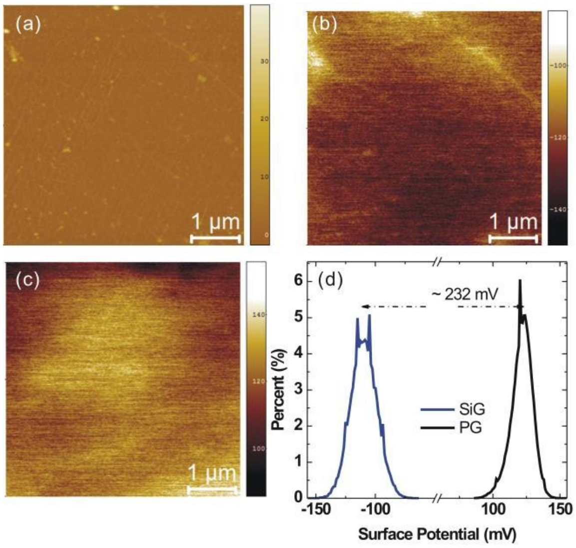

Fig. 5 (a) Topography and (b) surface potential map of SiG film. (c) Surface potential map of PG film. (d) Distribution of surface potential of SiG and PG film.

In order to investigate the effect of Si doping on the electrical properties of graphene, back-gated field effect transistors (FETs) based on PG and SiG films were fabricated by UV photolithography and measured in air at room temperature. Figure 6a shows the drain-source current (I_{ds}) versus voltage (V_{ds}) curve of s representative SiG FET under zero gate voltage (V_g=0). The linear I_{ds} versus V_{ds} curve indicates that the contact between metallic electrode and SiG film is ohmic. Figure 6b shows the typical transfer characteristics of PG and SiG FETs. The Dirac point for PG film is ~ + 63 V; in contrast, the Dirac point for SiG film is large than + 100 V. The upshift of Dirac point indicates that the silicon doping is p-type doping. Furthermore, the doping hole concentration (p) can be estimated from $p = \frac{C_0}{e} \Delta V_{\mathrm{Dirac}} \Big|_{\mathrm{PG}}^{\mathrm{SiG}}$, where C_0 is the back-gated capacitance with the value of 11.5 nF/cm^2, e is the electron charge, and $\Delta V_{\mathrm{Dirac}} \Big|_{\mathrm{PG}}^{\mathrm{SiG}}$ is the difference of Dirac points between SiG and PG film. As a consequence, we can get that the value of doping hole concentration caused by silicon doping is larger than 2.65×10^{12} cm^{-2}, which is consistent with above Raman studies.

Based on the above Raman, KPFM and electrical studies, we can confirm that silicon doping shows typical p-type doping characteristics. The corresponding doping mechanism can be explained by the following two reasons. (1) Doped silicon atoms: Theories calculation demonstrated that when the doped silicon content was lower than 16.6 at%，the Fermi level of SiG was lower than the middle of the gap, indicating p-type characteristics.[19] Furthermore, experiential report also revealed that doped silicon atoms caused the increase of hole concentration in nitrogen and silicon co-doped reduced graphene oxide.[31] (2) Absorbed O_2 molecules: It is well known that absorbed O_2 molecules can withdraw electrons from graphene, resulting p-type doping.[38,39] On the other hand, the above XPS studies reveal that more O_2 molecules are absorbed on SG than PG film, which is due to the doped Si-C structures with low absorption energy. Thus, besides doped silicon atoms, the absorption of O_2 molecules caused by silicon doping also contributes to the p-type doping for SG film.

In addition, the carrier mobilities (μ) of PG and SG films can be estimated as $\mu = g_m L / W C_0 V_{ds}$, where $g_{\mathrm{m}} = \mathrm{d}I_{\mathrm{ds}} / \mathrm{d}V_{\mathrm{g}} \Big|_{V_{\mathrm{ds}}=0.8\ \mathrm{V}}$ is obtained from Figure 6b; L and W are the length (40 μm) and width (6 μm) of graphene channel, respectively. The estimated room-temperature hole mobilities of PG and SG films are ~ 1135 and ~ 660 cm^2/Vs, respectively. The decrease of mobility caused by silicon doping is mainly due to the doped silicon atoms as scattering centres for carriers. However, we also notice that, the room-temperature carrier mobility value of SiG film is considerably high, which is close to the best value of reported nitrogen or boron doped graphene films synthesized by CVD method.[13,14,40] We believe that the silicon atoms doped into graphene with pure Si-C bonds (not the Si-O bonds) is important for the high mobility of our SiG film.

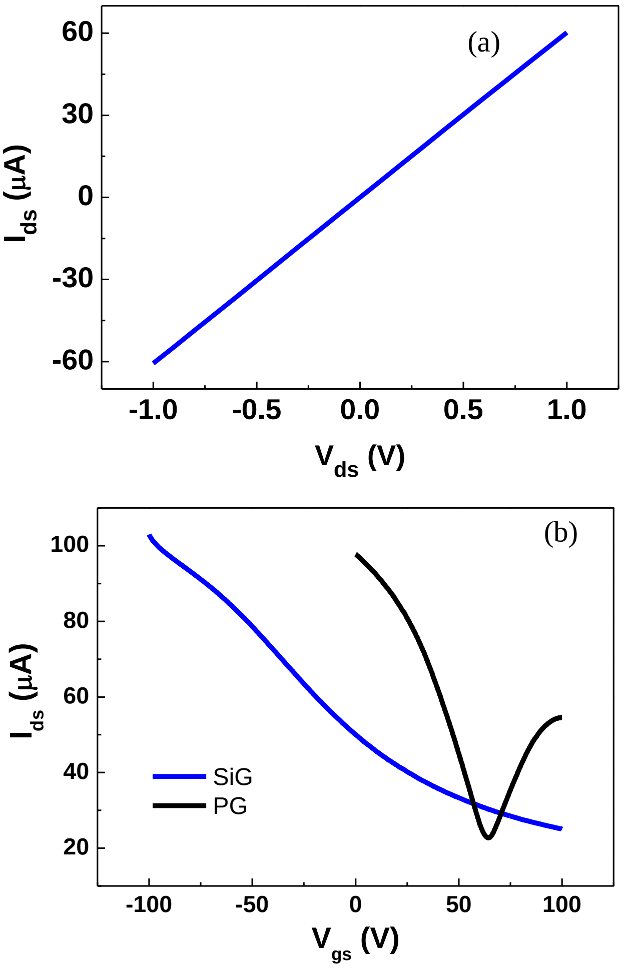

Fig. 6 (a) I_{ds}-V_{ds} plots of a typical SiG FET under V_g=0V. (b) Transfer characteristic of FETs based on PG and SiG films (V_{ds}=0.8V).

Conclusions

We have synthesized monolayer SiG film by using CVD method, where triphenylsilane was used as the sole carbon and silicon source. The XPS studies have confirmed that silicon atoms are doped into graphene, and revealed that the silicon content is ~ 2.63 at%. More significantly, the silicon atoms are incorporated into the graphene lattice with the single doping structure of Si-C bonds. Furthermore, Raman, KPFM and Raman, KPFM and electrical studies all reveal that silicon doping is p-type doping. In addition, electrical studies indicate that the as-synthesized SiG film has a considerably high carrier mobility of about 660 cm^2/Vs at room temperature. We are convinced that the SiG film not only will be widely used in electrical devices, but also can serve as an excellent platform for studying silicon doping effects on the physical and chemical properties of graphene due to its single doping structure of Si-C bonds.

Acknowledgements

The research was supported by the National Natural Science Foundation of China (Grant Nos. 51202022, 51372033 and 61378028), the Specialized Research Fund for the Doctoral Program of Higher Education (Gran No. 20120185120011), the 111 Project (Grant No. B13042), Sichuan Youth Science and Technology Innovation Research Team Funding (Grant No. 2011JTD0006), the International Science and Technology Cooperation Program of China (Gran No. 2012DFA51430), and the Sino-German Cooperation PPP Program of China.

Notes and references

[a] *State Key Laboratory of Electronic Thin Films and Integrated Devices, University of Electronic Science and Technology of China,Chengdu 610054, P. R. China. Fax:+86-028-83202710; Tel: +86-028-83202710; E-mail: lipingjian@uestc.edu.cn*

[a] *State Key Laboratory of Electronic Thin Films and Integrated Devices, University of Electronic Science and Technology of China,Chengdu 610054, P. R. China. Fax:+86-028-83202710; Tel: +86-028-83202710; E-mail: yfchen@uestc.edu.cn*

[b] *Interdisciplinary Nanoscience Center (iNANO), Aarhus University, DK-8000 Aarhus C, Denmark*

[c] *Department of Engineering, Aarhus University, DK-8000 Aarhus C, Denmark*

1. K. S. Novoselov, A. K. Geim, S. V. Morozov, D. Jiang, Y. Zhang, S. V. Dubonos, I. V. Grigorieva and A. A. Firsov, *Science*, 2004, **306**, 666.
2. L. B. Gao, G. X. Ni, Y. P. Liu, B. Liu, A. H. Castro Neto and K. P. Loh, *Nature*, 2014, **505**, 190.
3. Y. B. Zhang, Y. W. Tan, H. L. Stormer, P. Kim, *Nature*, 2005, **438**, 201.
4. Z. G. Wang, P. J. Li, Y. F. Chen, X. Hao, J. B. Liu, R. Huang and Y. R. Li, *ACS Nano*, 2011, **5**, 7149.
5. I. Meric, M. Y. Han, A. F. Young, B. Ozyilmaz, P. Kim and K. L. Shepard, *Nat. Nanotechnol.*, 2008, **3**, 654.
6. K. Chen, X. Wan and J. B. Xu, *J. Mater. Chem. C*, 2013, **1**, 4869.
7. H. B. Wang, T. Maiyalagan and X. Wang, *ACS Catal.*, 2012, **2**, 781.
8. J. M. Yun, S. Park, Y. H. Hwang, E. Lee, U. Maiti, H. Moon, B. Kim, B. Bae, Y. Kim and S. O. Kim, *ACS Nano*, 2014, **8**, 650.
9. Y. F. Lu, S. T. Lo, J. C. Lin, W. J. Zhang, J. Y. Lu, F. H. Liu, C. M. Tseng, Y. H. Lee, C. T. Liang and L. J. Li, *ACS Nano*, 2013, **7**, 6522.
10. Z. G. Wang, P. J. Li, Y. F. Chen, J. B. Liu, H. J. Tian, J. H. Zhou, W. L. Zhang and Y. R. Li, *J. Mater. Chem. C*, 2014, **2**, 7396.
11. Z. Jin, J. Yao, C. Kittrell and J. M. Tour, *ACS Nano*, 2011, **5**, 4112.
12. Y. B. Tang, L. C. Yin, Y. Yang, X. H. Bo, Y. L. Cao, H. E. Wang, W. J. Zhang, I. Bello, S. T. Lee, H. M. Cheng and C. S. Lee, *ACS Nano*, 2012, **6**, 1970.
13. H. Wang, Y. Zhou, D. Wu, L. Liao, S. L. Zhao, H. L. Peng and Z. F. Liu, *Small*, 2013, **9**, 1316.
14. J. Zhang, J. J. Li, Z. L. Wang, X. N. Wang, W. Feng, W. Zheng, W. W. Cao and P. A. Hu, *Chem. Mater.*, 2014, **26**, 2460.
15. Z. G. Wang, P. J. Li, Y. F. Chen, J. R. He, W. L. Zhang, O. G. Schmidt and Y. R. Li, *Nanoscale*, 2014, **6**, 7281.
16. Y. G. Zhou, P. Yang, Z. G. Wang, H. Y. Xiao, X. T. Zu, X. Sun, M. A. Khaleel and F. Gao, *Appl. Phys. Lett.*, 2011, **98**, 093108.
17. D. Kaplan, V. Swaminathan, G. Recien, R. Balu and S. Krna, *J. Appl. Phys.*, 2013, **113**, 183701.
18. S. K. Mudedla, K. Balamurugan and V. Subramanian, *J. Phys. Chem. C*, 2014, **118**, 16165.
19. M. S. Sharif Azadeh, A. Kokabi, M. Hosseini and M. Fardmanesh, *Micro Nano Lett.*, 2011, **6**, 582.
20. Y. Chen, Y. J. Liu, H. X. Wang, J. X. Zhao, Q. H. Cai, X. Z. Wang and Y. H. Ding, *ACS Appl. Mater. Interfaces*, 2013, **5**, 5994.
21. P. Zhang, X. L. Hou, J. L. Mi, Y. Q. He, L. Lin, Q. Jiang, M. D. Dong, *Phys. Chem. Chem. Phys.*, 2014, **16**, 17479.
22. W. Zhou, J. Lee, J. Nanda, S. T. Pantelides, S. J. Pennycook and J. C. Idrobo, *Nat. Nanotechnol.*, 2012, **7**, 161.
23. W. Zhou, M. D. Kapetanakis, M. P. Prange, S. T. Pantelides, S. J. Pennycook and J. C. Idrobo, *Phys. Rev. Lett.*, 2012, **109**, 206803.
24. Q. M. Ramasse, R. Zan, U. Bangert, D. W. Boukhvalov, Y. W. Son and K. S. Novoselov, *ACS Nano*, 2012, **6**, 4063.
25. R. T. Lv, M. C. dos Santos, C. Antonelli, S. M. Feng, K. Fujisawa, A. Berkdemir, R. Cruz-Silva, A. L. Elias, N. Perea-Lopez, F. Lopez-Urias, H. Terrones and M. Terrones, Adv. Mater., 2014, 26, 7593.
26. H. Watanabe and T. Hosoi, Fundamental Aspects of Silicon Carbide Oxidation, Physics and Technology of Silicon Carbide Devices, 2012, ISBN: 978-953-51-0917-4, InTech, DOI: 10.5772/51514. Available from: http://www.intechopen.com/books/physics-and-technology-of-silicon-carbide-devices/fundamental-aspects-of-silicon-carbide-oxidation
27. N. Alderman, L. Danos, M. C. Grossel and T. Markvart, *RSC Adv.*, 2013, **3**, 20125.
28. G. Riveros, S. Meneses, S. Escobar, C. Garin and B. Chornik, *J. Chil. Chem. Soc.*, 2010, **55**, 61.
29. X. Wang, Q. H. Weng, X. Z. Liu, X. B. Wang, D. M. Tang, W. Tian, C. Zhang, W. Yi, D. Q. Liu, Y. Bando and D. Golberg, Nano Lett., 2014, 14, 1164.
30. L. T. Qu, Y. Liu, J. Baek and L. M. Dai, ACS Nano, 2010, 4, 1321.
31. F. Niu, J. M. Liu, L. M. Tao, W. Wang and W. G. Song, *J. Mater. Chem. A*, 2013, **1**, 6130.
32. C. H. Zhang, L. Fu, N. Liu, M. H. Liu, Y. Y. Wang and Z. F. Liu, Adv. Mater., 2011, 23, 1020.
33. A. Das, S. Pisana, B. Chakraborty, S. Piscanec, S. K. Saha, U. V. Waghmare, K. S. Novoselov, H. R. Krishnamurthy, A. K. Geim, A. C. Ferrari and A. K. Sood, *Nat. Nanotechnol.*, 2008, **3**, 210.
34. L. G. Cancado, K. Takai, T. Enoki, M. Endo, Y. A. Kim, H. Mizusaki, A. Jorio, L. N. Coelho, R. Magalhaes-Paniago and M. A. Pimenta, *Appl. Phys. Lett.*, 2006, **88**, 163106.
35. H. Gao, Z. Liu, L. Song, W. H. Guo, W. Gao, L. J. Ci, A. Rao, W. J. Quan, R. Vajtai and P. M. Ajayan, Nanotechnology, 2012, 23, 275605.

36. Y. J. Yu, Y. Zhao, S. M. Ryu, L. E. Brus, K. S. Kim and P. Kim, *Nano Lett.*, 2009, **9**, 3430.
37. O. Ochedowski, B. Kleine Bussmann and M. Schleberger, *Sci. Rep.*, 2014, **4**, 6003.
38. S. H. Park, J. M. Chae, M. H. Cho, J. H. Kim, K. H. Yoo, S. W. Cho, T. G. Kim and J. W. Kim, *J. Mater. Chem. C*, 2014, **2**, 933.
39. Y. Ogawa, K. Komatsu, K., M. Tsuji, K. Tsukagoshi and H. Ago, *Nanoscale*, 2014, **6**, 7288.
40. T. R. Wu, H. L. Shen, L. Sun, B. Cheng, B. Liu and J. C. Shen, New J. Chem., 2012, 36, 1385.

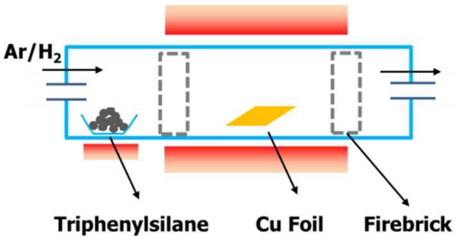

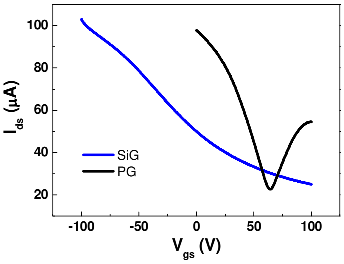

Silicon-doped graphene film was synthesized by CVD using triphenylsilane as sole carbon and silicon sources. The silicon-doped graphene exhibits strong p-type feature and has a large hole mobility of 660 cm^2/Vs.